Nuclear Materials and Energy 12 (2017) 1303–1307

Contents lists available at ScienceDirect

Nuclear Materials and Energy

journal homepage: www.elsevier.com/locate/nme

Damage and deuterium retention of re-solidified tungsten following vertical displacement event-like heat load

Y. Hamaji[a,*], H.T. Lee[b], A. Kreter[c], S. Möller[c], M. Rasinski[c], M. Tokitani[a], S. Masuzaki[a], A. Sagara[a], M. Oya[b], K. Ibano[b], Y. Ueda[b], R. Sakamoto[a]

[a] National Institute for Fusion Science, National Institutes of Natural Sciences, 322-6 Oroshi-cho, Toki 509-5292, Japan
[b] Graduate School of Engineering, Osaka University, 2-1 Yamadaoka, Suita 565-0871, Japan
[c] Forschungszentrum Jülich GmbH, Institut für Energie- und Klimaforschung - Plasmaphysik, 52425 Jülich, Germany

ARTICLE INFO

Article history:
Received 12 July 2016
Revised 16 October 2016
Accepted 2 November 2016
Available online 22 November 2016

Keywords:
Tungsten
Retention
Melting
Divertor
High heat flux
NRA

ABSTRACT

Surface morphology and hydrogen isotope retention of W specimen melted with vertical displacement event-like heat load and subsequent deuterium (D) plasma exposure were studied. Applied heat loads using electron beam without raster scanning were about 190 and 230 MW/m^2 in heat flux and 0.08, 0.12 and 0.16 s in duration. After the heat load application, specimens showed apparent melting spots with grain growth or dense micrometer scale convex structure. Cracks were observed only in the part with the convex structure. D retention in the melted part of specimens was not significantly larger than in the reference specimen despite large changes of surface characteristics.

1. Introduction

Tungsten (W) has good physical properties such as high thermal conductivity, low hydrogen isotope retention, and low sputtering yield by light species. Therefore, W has been used as a plasma facing material in current devices and will be used as plasma facing components in future devices such as ITER and beyond. However, as a metallic material, surface melting and microstructure changes in the bulk due to extreme heat flux is a serious concern. Surface changes in dimensions or properties can adversely affect plasma operation, while bulk changes can shorten the component lifetime. In addition, T retention strongly depends on materials' surface and bulk properties. Therefore, material degradation due to excessive heat loads may play an important role in Tritium (T) retention in W with its impact on safety.

Heat flux to W components in normal operations in fusion devices will be controlled below the melting threshold of W. However, heat load in off-normal events such as unmitigated Edge localized mode (ELM), Vertical displacement event (VDE), and disruptions might exceed the melting threshold. VDE is due to unintentional vertical movement of core plasma. The estimated heat flux to plasma facing components during VDE strongly depends on the scenario of the event. For ITER, heat flux greater than 120 - 600 MW/m^2 is estimated [1]. In general, most estimates indicate the time duration of VDE is longer (typically $>$ 100 ms [2–4]) than other fast transient heat loads like ELMs or thermal/current quenches during disruptions ($<$ 1 ms). Thus, unlike these fast transient events in which heat deposition is limited to near surface [5] (thermal diffusion length of W in 1 ms is about 0.5 mm), VDE may cause more severe macroscopic melting due to the longer duration. Previous studies [6–9] have examined W melting under conditions of where the surface temperature, and temperature gradient in the material was decided by the heat removal capability of the components due to the longer heat load. However, actual temperature gradient in material during VDE is steeper than that because of shorter duration (thermal diffusion length in 0.1 sec. is about 5 mm in W). The temperature gradient may cause the more residual stress after the heat load. In this study, the impact of VDE-like heat load on surface morphology and corresponding impact on hydrogen isotope retention was investigated in realistic time scale.

2. Experimental

99.99% pure polycrystalline W manufactured by A.L.M.T. Corp. Japan were used. The specimen was 5 mm in height, but was the shape of a two level cake. The top part was 2 mm in height and 5 mm in diameter, while the bottom part was 3 mm in height

* Corresponding author.
E-mail addresses: hamaji.yukinori@nifs.ac.jp, nrd36502@gmail.com (Y. Hamaji).

http://dx.doi.org/10.1016/j.nme.2016.11.003

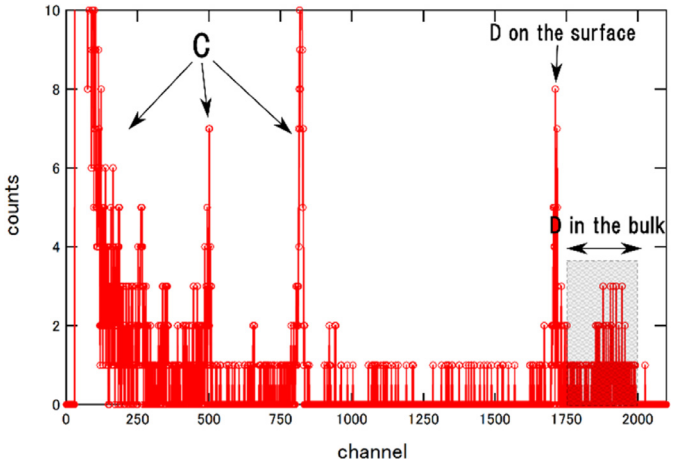

Fig. 1. A typical NRA spectrum in this study. The shaded part of the spectrum is the part integrated to estimate D retention in the bulk.

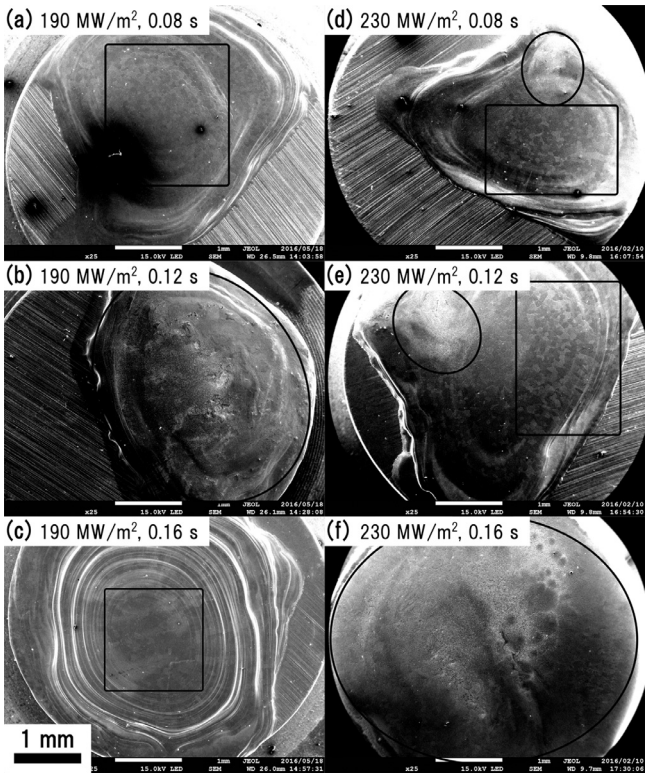

Fig. 2. Images of a specimen irradiated by e-beam. Irradiated conditions of each specimens are noted in the images.

and 7 mm in diameter. The specimens were exposed to VDE-like heat loads using an electron beam (e-beam) facility called Active Cooling Test stand 2(ACT2) at National institute for fusion science, Japan [10]. The beam profile was Gaussian-like with a FWHM of 9 mm as measured by electrostatic probes. One specimen was placed in a specimen holder made of graphite without any mask or jig. The beam diameter was larger than the specimen, which allowed for the focused electron beam to irradiate the entire specimen without raster scanning. The beam was translated between a beam dump and the specimen by electromagnetic deflection lenses at translation speeds greater than 500 m/s at 1.5 mm resolution. However, part of the e-beam also heated up the surrounding graphite holder resulting in carbon sublimation – the issue of C contamination is addressed in Section 3. The specimen holder was electrically isolated and a positive 50 V bias voltage applied to collect secondary and thermal electrons. Absorbed heat flux was controlled to be 190 and 230 MW/m^2 at the center of the beam. This was calculated from the output power of the e-beam, beam profile, and absorption coefficient. Output power of the e-beam was determined from the acceleration voltage (40 kV) and the current measured during irradiation of pure graphite. Absorption coefficient was calculated by reflection coefficient (about 48%) and energy deposition by the reflected electrons estimated from ref [11]. (about 73% of "reflected" electrons). The pulse duration was 0.08, 0.12 and 0.16 seconds, respectively. The base temperature prior to e-beam irradiation for all specimens was 300 K.

Next, melted specimens were exposed to D plasma in the linear plasma device PSI-2, at Juelich Forschungszentrum, Germany [12]. The incident energy, flux, fluence and implantation temperature were 40 eV, 8×10^{21} D/m^2/s, 1×10^{26} /m^2, and 473 K, respectively. The samples were exposed to D plasma over a course of two days. In the first day, three specimens melted under 190 MW/m^2 heat load (0.08, 0.12 and 0.16 s) along with a reference specimen was simultaneously exposed to the D plasma. The second day consisted of repeating the experiments with specimens melted under 230 MW/m^2 heat loads.

To measure the C and D content following D plasma exposures, nuclear reaction analysis (NRA) was performed using a 2.94 MeV ^{3}He beam. Detected reactions were D(^{3}He,p)^{4}He and ^{12}C(^{3}He,p)^{14}N. The cross sections of the reactions were taken from the literature [13,14]. The diameter of the probe helium beam was about 1 mm. Measurements were performed on both melted and unmelted regions when possible. For each measurement, signal counts were standardized by RBS (Rutherford backscattering spectrometry) signal. A typical NRA spectrum is shown in Fig. 1. The three peaks observed below channel 1000 correspond to Carbon. While, the peaks observed above channel 1500 correspond to D. The D signal can be separated into two peaks – labeled "D on the surface" and "D in the bulk". The "D on the surface" corresponds to D trapped at the near surface (< 50 nm) while the "D in the bulk" corresponds to D retention up to $\sim$3 μm after which the cross section of the reaction decreases rapidly. The spectra of the near surface C and D peaks were fitted by SIMNRA code [15] to obtain values of C and D areal density, respectively. Due to limitation in measurement time, the signal from D in the bulk is statistically poor, and was not fitted using SIMNRA. However, bulk retention is important for this study since the thickness of the melted layers were much greater than 3 μm. Therefore, in order to roughly estimate the D areal density in the bulk region, we integrated the spectra between 11,480 and 13,133 keV (corresponding to channels 1725 to 2000). The integrating window is indicated as the shaded region in Fig. 1. It should be noted that this integrated value is not applicable for quantitative estimation but only for comparison between specimens.

Surface modification of the specimens were observed using SEM (scanning electron microscope), FIB(focused ion beam)-SEM, and EDX(Energy Dispersive X-ray spectroscopy). In FIB-SEM observation, in order to observe the surface clearly and to protect the surface from the ion bombardment of FIB, carbon (C) layer (e.g. black layer shown in the Fig. 3(d-f)) and W layer (white layer on the C layer) were deposited. Images of cross sections in this paper were taken at an incident angle of 32 ° to the surface.

3. Results and discussion

3.1. Surface morphology changes due to heat load

Fig. 2 consists of SEM images following exposure at 190 MW/m2 (a-c) and 230 MW/m2 (d-f) for various e-beam duration

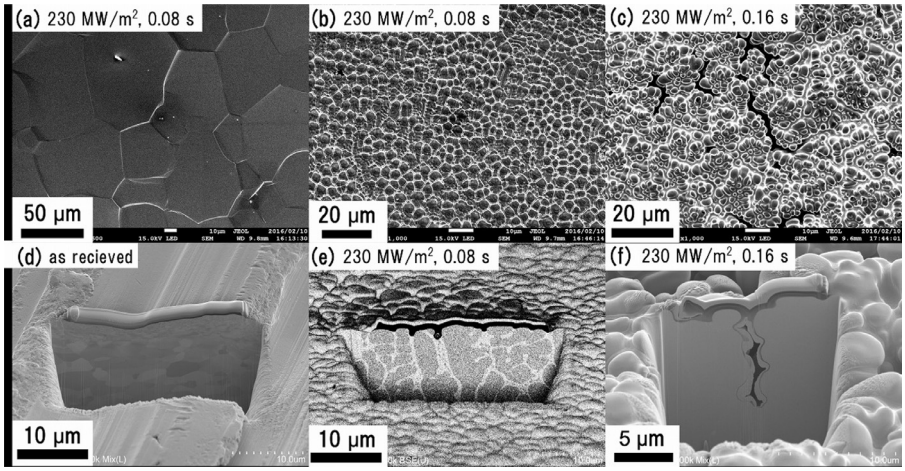

Fig. 3. (a)(b)(c): Surface SEM image of specimen. (d): Cross sectional image of as-received specimen (without e-beam and D ion irradiation). (e): Cross sectional image taken by backscattered electron of a globular-like structure. (f): Cross sectional image of a crack.

(0.08, 0.12 and 0.16 s). The melted region and unmelted region can be clearly distinguished for all irradiation cases except for the highest heat load case. The original rough surface preparation by mechanical polishing is also visible as seen by the parallel scratch marks. Due to the limited resolution for transversal control of the e-beam (about 1.5 mm), the center of the melted areas does not correspond to the center of the specimens. Such misalignment resulted in relatively severe melting of the edge of specimens for a few cases (e.g., upper part of Fig. 2(a) or (b)). Two types of surface morphology were observed in the melted region. The first is visible grains/ grain growth as seen in Fig. 2(a), (c), (d), and (e)(as seen in the black squares). The second is a surface roughening without visible grains as illustrated by the entire melted region in Fig. 2(b) and (f) or in certain areas as seen in Fig. 2(d) and (e) (as seen in the black circles).

Fig. 3 shows higher magnification and cross-sectional SEM images of structures discussed above. Fig. 3 (a-c) consists of the surface images of irradiated specimens. Fig. 3(d-f) consists of the cross-sectional images of specimens. Irradiation conditions of specimens shown in Fig. 3 are indicated on each figure. The visible grains were typically more than 50 micrometers wide as shown in fig. 3(a). These large grains indicate grain growth during or after re-solidification since the original grain size was less than one micrometer at the surface and several micrometers in the bulk (see fig. 3(d)). In Fig. 3(b), a close-up image of the rough surface without visible grains is shown, which corresponds to the circled area in Fig. 2(d). The higher magnification reveals complex “convex” surface structures that are several micrometers in scale. This structure was also reported in a study regarding W exposed to TEXTOR’s edge plasma as “globular-like structures” [7]. Fig 3(e) shows a backscattered electron image of the cross section of the globular-like structure shown in Fig. 3(b). The depths of the concavities of the globular-like structure were about 1 μm. Interestingly, contrast in the regions between the globular-like structures was seen. In general, brightness in backscattered electron images reflects differences in composition, internal stress, or defects in the material. The mechanism behind the formation of such globular-like structures and the reason behind the contrast between the structures are still unclear. It may be noted that specimen irradiated for 0.16 s with 190 MW/m^2 did not show such structures although the specimen irradiated for 0.12 s showed the globular-like structure. The specimen irradiated for 0.12 s received the e-beam at the edge of the specimen due to misalignment. E-beam irradiation on the edge induces higher peak temperature and heavier melting due to limitation of thermal diffusion direction. There is a possibility that melting of the edge specimen and the resulting higher temperatures may have contributed to the formation of the globular structure (i.e. residual of boiling). Another possibility is the influence of C impurity. C impurities may prevent grain growth during re-solidification by forming eutectic structures. However, no significant C impurity was found in EDX measurement from the cross section of the globular-like structure (Fig 3(e)). This indicates that the amount of C impurity was smaller than detection limit of EDX. The amount of surface C impurity was also comparable to reference samples measured using NRA.

In case of specimens irradiated with 230 MW/m^2 for 0.12 and 0.16 s and 190 MW/m^2 for 0.12 s, cracks were observed in the melted regions containing the globular-like structure as shown in Fig. 3(c). Fig. 3(f) shows the cross sectional view of one of these cracks. The crack is partially filled with C and W layers due to the deposition layers deposited during the digging process by focused ion beam. The depth of this crack was about 10 μm. Interestingly, cracks were only observed in regions containing the globular-like structures. This suggests that crack formation was enhanced by formation of the globular-like structure.

3.2. Blistering by D ion bombardment

Fig. 4 shows the SEM images of blisters formed by D plasma exposure in specimens irradiated at 230 MW/m^2 for various e-beam hold time. Qualitatively, in case of specimen irradiated for 0.08 s (Fig. 3(a)), very few blisters were observed in regions of visible grain growth or regions containing globular-like structure. However with increasing irradiation time, the number of blisters increased (see Fig. 4(b) and 4(c)). At present it is difficult to compare the density of blisters between regions with and without globular-like structures. A more detailed image analysis of the surfaces is required.

3.3. D and C surface and bulk retention

Fig. 5 shows the surface areal density of C on melted and unmelted regions plotted against e-beam hold time. C areal density of reference specimen without e-beam irradiation is shown as a dotted line. Open symbols and filled symbols correspond to melted and unmelted regions, respectively. C areal density measured on the reference specimen corresponds to typical C contamination levels. Slightly higher C density in unmelted regions and in the melted regions were measured but still correspond to contamination levels. In the case of unmelted region of the specimen irradi-

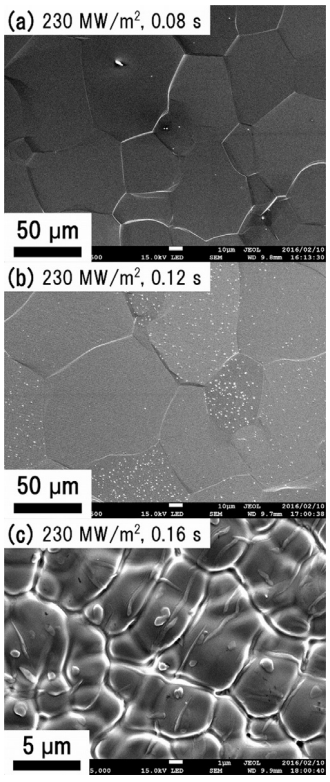

Fig. 4. Blisters observed on a specimen irradiated for 0.08 s (a), 0.12 s (b) and 0.16 s (c) with 230 MW/m^2.

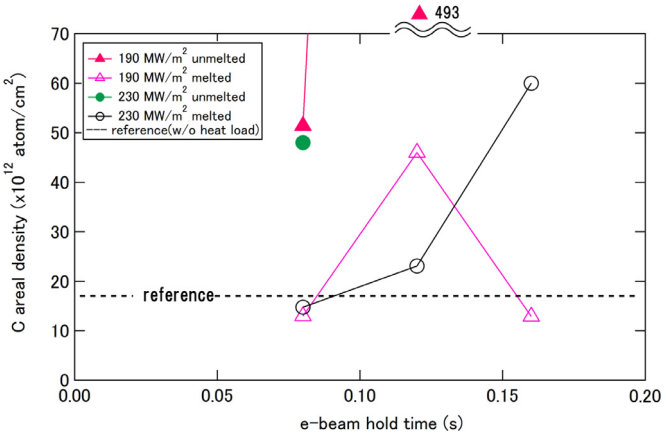

Fig. 5. C areal density of specimens measured by NRA. The absolute value were obtained by SIMNRA code. C areal density of a reference (not irradiated) specimen is shown as black dotted line.

ated for 0.12 s at 190 MW/m^2, C areal density is one order of magnitude higher than others due to the misalignment of e-beam and resulting C sublimation. The specimens containing the globular-like structures generally showed a slight increase in C areal density (0.12 s with 190 MW/m^2, and 0.16 s with 230 MW/m^2). In the ITER-like wall experiment at JET, significant amount of C was observed in divertor tiles likely from the residual C remaining from the transition from C tiles [16]. Nevertheless, the absolute value of C impurities was not reported in [16] nor is such values well known for future devices. Thus if C impurities aid in the formation of globular-like structures, then there is a possibility that such structures will also form in JET or future devices under unmitigated heat flux loads.

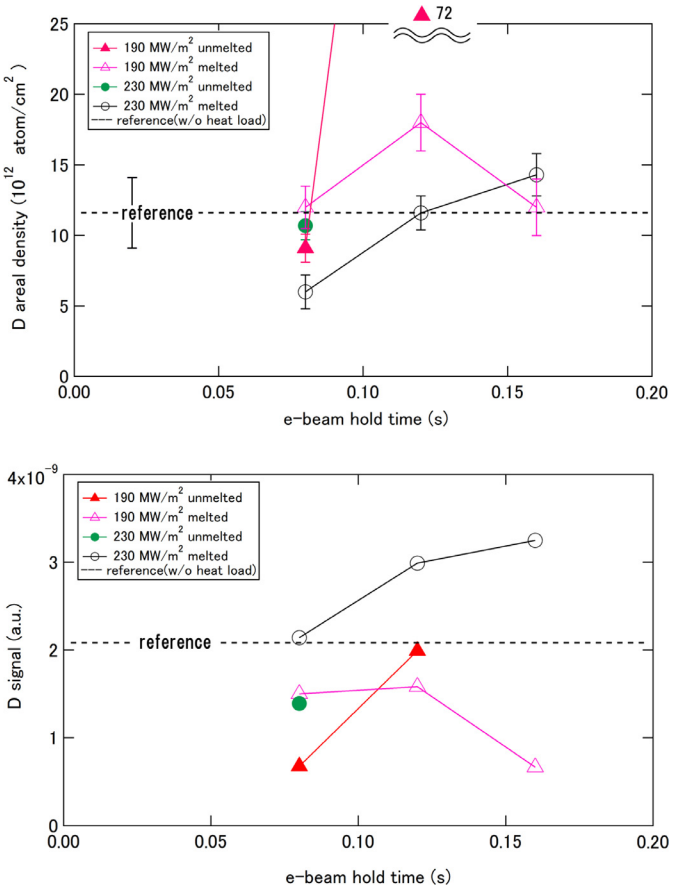

Fig. 6. (a): D areal density obtained by NRA on the surface. (b): Integrated value of the signal from retained D in the bulk calculated using the method described in Section 2. Values of reference (not irradiated) specimen are shown as black dotted line.

Fig. 6(a) shows the surface D areal density as function of e-beam hold time. D areal density of the reference specimen was shown as dotted line. In the case of 0.08 s irradiation with190 MW/m^2 and 230 MW/m^2, D areal densities were roughly the same or slightly smaller than reference specimen despite larger C areal density in some of the regions. This decrease is likely due to the thermal annealing of defects formed during preparation/cutting process. In the case of melted regions for specimens irradiated with 230 MW/m^2, D retention increased with increasing e-beam hold time. This increase indicates possible generation of additional trap sites in the near surface due to melting. However, the increase in D retention is modest and within a factor of two. Significantly larger D areal density of melted and unmelted regions for specimen irradiated at 0.12 s with 190 MW/m^2 is likely due to surface C impurities. In the case of specimens irradiated for 0.12 and 0.16 s with 230 MW/m^2, C density increased with increasing e-beam irradiation time in melted regions. A corresponding increase in D areal density was also observed so we cannot at present eliminate the effect of C on the increase in D retention.

Fig 0.6 (b) shows the integrated signal that correlates to D trapped in the bulk. T signal of the reference specimen was shown as dotted line.Only melted regions of specimens irradiated with 230 MW/m^2 showed more retention in the bulk compared with reference specimens. Less bulk D retention suggests defects recovery by annealing and re-solidification. The globular-like structure and C impurity should not be the reason of increase of specimens with 230 MW/m^2 because melted region in the specimen irradiated for 0.12 s with 190 MW/m^2 did not show significant increase.

The increase might be due to the effect of microstructural changes induced by melting and re-solidification in the bulk. More detailed inspection such as TEM (Transmission electron microscopy) observation or measurement of composition in the bulk are required to confirm the origin of these trap sites. However, the increase of D signal from the bulk of melted region are 1.5 times larger than that of reference specimen. The effect of melting and the surface modification on D retention at surface is not drastic in view of the significant changes to surface morphology. In addition, since VDEs melt only limited areas of the exposed surfaces of components, our results suggests that the effect of melting on D retention in actual large devices would be limited in comparison to effects of impurities like nitrogen or carbon.

4. Summary

In this paper, surface morphology and hydrogen isotope retention of W specimens melted with VDE-like heat load were studied. Applied heat loads using e-beam were about 190 and 230 MW/m^2 in heat flux and from 0.08, 0.12 and 0.16 s in duration. There were regions with clear grain growth and with “globular-like structure” in melted parts of the specimens. The globular-like structure is a dense convex structure that was about 2–3 μm wide and 1 μm in height. The globular-like structure may arise from melting of the edge of the specimens or C impurity introduced during e-beam irradiation. Cracks were only observed in regions with the globular-like structure.

Melted specimens were exposed to D plasma in linear plasma device PSI-2. After D plasma exposure, D retention on the surface and bulk were estimated using nuclear reaction analysis. Melted regions showed roughly the same D retention on the surface compared with reference (without e-beam irradiation) specimen except the specimen with extremely high C contamination due to accidental misalignment of e-beam irradiation. In the bulk, an increase in D retention in melted regions in specimens irradiated with 230 MW/m^2 was observed. This suggests that additional trap sites may be generated by microstructural changes due to unmitigated heat loads. However, the increase was within a factor of two. The results of this study suggest that the effect of VDE-like heat load on the D retention was not significant. However, melting might induce unique surface morphology and enhance crack formation. In addition, melting enhancement effect of simultaneous ion bombardment was reported [17]. Therefore, further investigation of effect of melting and synergetic effect is required.

Acknowledgements

The research was carried out within the framework of International Energy Agency Plasma Wall Interaction Technology Collaboration Programmes (IEA PWI TCP). One of the authors (H. T. Lee) acknowledges travel funding from this program. This work was also supported by NIFS research budget (code ULFF032).

References

[1] A. Hassanein, V. Sizyuk, et al., Can tokamaks PFC survive a single event of any plasma instabilities? J. Nucl. Mater. 438 (2013) S1266–S1270.
[2] M. Lehnen, G. Arnoux, et al., Disruption heat loads and their mitigation in JET with the ITER-like wall, J. Nucl. Mater. 438 (2013) S102–S107.
[3] M. Sugihara, M. Shimada, et al., Disruption scenarios, their mitigation and operation window in ITER, Nucl. Fusion. 47 (2007) 337–352.
[4] A. Hassanein, T. Sizyuk, et al., Vertical displacement events: a serious concern in future ITER operation, Fusion Eng. Des. 83 (2008) 1020–1024.
[5] G. Arnoux, J. Coenen, et al., Thermal analysis of an exposed tungsten edge in the JET divertor, J. Nucl. Mater. 463 (2015) 415–419.
[6] J.W. Coenen, V. Philipps, et al., Analysis of tungsten melt-layer motion and splashing under tokamak conditions at TEXTOR, Nucl. Fusion. 51 (2011) 083008.
[7] G. Sergienko, B. Bazylev, et al., Experience with bulk tungsten test-limiters under high heat loads: melting and melt layer propagation, Phys. Scr. T128 (2007) 81–86.
[8] J.W. Coenen, V. Philipps, et al., Melt-layer ejection and material changes of three different tungsten materials under high heat-flux conditions in the tokamak edge plasma of TEXTOR, Nucl. Fusion. 51 (2011) 113020.
[9] J.W. Coenen, B. Bazylev, et al., Tungsten melt layer motion and splashing on castellated tungsten surfaces at the tokamak TEXTOR, J. Nucl. Mater. 415 (2011) S78–S82.
[10] Y. Hamaji, M. Tokitani, et al., ACT2: a high heat flux test facility using electron beam for fusion, Plasma Fusion Res. 11 (2016) 1–4 2405089.
[11] I.S. Tilinin, Reflection of fast electrons normally incident on a free film surface, Phys. Chem. Mech. Surf. 5 (1989) 476.
[12] B. Schweer, G. Sergienko, et al., Linear plasma device PSI-2 for plasma-material interaction, Fusion Sci. Technol. 68 (2015) 8–14.
[13] V.K. Alimov, M. Mayer, et al., Differential cross-section of the D(^{3}He,p)^{4}He nuclear reaction and depth profiling of deuterium up to large depths, Nucl. Instruments Methods Phys. Res. Sect. B 234 (2005) 169–175.
[14] H.M. Kuan, T.W. Bonner, et al., An investigation of the $C^{12}+He^3$ reactions at bombarding energies between 1.8 and 5.4 MeV, Nucl. Phys. 51 (1964) 481–517.
[15] M. Mayer, SIMNRA User’s Guide, IPP, Max Planck-Institut Fur Plasmaphys, 1997 Tech. Rep. 9/113.
[16] J.P. Coad, E. Alves, et al., Surface analysis of tiles and samples exposed to the first JET campaigns with the ITER-like wall, Phys. Scr. T159 (2014) 014012.
[17] G. De Temmerman, T.W. Morgan, et al., Effect of high-flux H/He plasma exposure on tungsten damage due to transient heat loads, J. Nucl. Mater. 463 (2015) 198–201.